Atmospheric Ice Accretion on Railway Overhead Powerline Conductors- A Numerical Case Study

A Lotfi[1]*, M S Virk[1], J A Pettersen[2]

1. Arctic Technology & Icing Research Group, UiT – The Arctic University of Norway

2. Department of Industrial Engineering, UiT – The Arctic University of Norway

ABSTRACT

Ice accretion on railway overhead contact wires/conductors can cause various critical operational and safety issues such as overloading, arc formation, mass imbalance, and wire galloping. The focus of this multiphase numerical study is to understand and analyze the ice accretion physics on railway overhead powerline conductors at various operating conditions. In this regard, two different geometric shape conductors of 12 mm diameter, 1) a grooved shape contact wire (like an actual railway conductor); 2) a standard circular shape contact wire are used. Computational Fluid Dynamics (CFD) based numerical simulations are carried out for both geometric configurations at different operating parameters such as wind speed, Liquid Water Content (LWC), cloud droplet size distribution, Median Volume Diameter (MVD), and atmospheric temperature. Analysis shows that variation in the operating weather parameters for both geometric configurations considerably affect the ice accretion, both in terms of accreted ice thickness and mass.

1. INTRODUCTION

Atmospheric ice can affect the safety, accessibility, economic efficiency, and infrastructure of transportation systems in many countries that experience harsh winters and extreme cold. In some railway areas like Norway, Sweden Finland, USA, Russia and Canada, the atmospheric temperature can drop to -35°C, which leads to ice and can affect the safety of railway operations [1, 2]. Many aspects of the impact of ice intensity variation due to climate change on railway infrastructure are still unclear for experts, managers, and maintenance organizations [3]. The most frequent challenges regarding the effects of ice on railway infrastructure are listed in Table 1.

An essential component of electrified railroads is the overhead contact wire system. This system supplies electricity for train traction and the quality of the locomotive's current collection directly depends on the pantograph's interaction with the catenary system [13]. Ice accretion on railway overhead catenary wires is a common wintertime cause of equipment malfunction and the train delays in cold regions [14]. Icing on railway overhead power lines can put the network's safety and reliability in danger, for instance, a long period of icing event can lead to power outages and tower collapse. Icing on railway contact wires can also cause

*Corresponding Author: arefeh.lotfi@uit.no

overloading, arc formation, mass imbalance, and wire galloping (low-frequency oscillation of wires), which are critical issues for engineers and researchers [15-17]. Figure 1 shows failure of overhead lines in presence of ice in Slovenia railway.

Table 1: Possible issues due to snow and ice on railway infrastructure [4-12].

Railway infrastructure issues related to icing	**Signaling system**	Icing on overhead power lines, pantographs, and third rails
		Malfunctioning of switches and turns due to freezing ice
		Trackside equipment like substation traction power
	Track	Ice accumulation on rail tracks
		Cracking rail
		Material failure of sleepers and railway track due to low temperatures
		Rockfall on tracks
		Tunnel icing, particularly at the entrance
	Platforms, stations, and parking spaces	
	More frequent and costly maintenance	

Figure 1: Example of icing on railway overhead lines [18].

Icing on overhead contact wires can be classified as glaze, granular rime, crystalline rime, wet snow, and mixed rime [16]. Atmospheric icing on contact wires occurs in conditions, where the cooling of an air mass causes the supercooling of the water droplets. Water droplets in the earth's atmosphere can remain in the liquid state at air temperature as low as -40°C, before spontaneous freezing occurs. The rate of atmospheric ice accretion on a structure is governed by two processes; a) the impingement of supercooled water droplets on the structure surface, and b) the surface thermodynamics, which determines what portion of the water impingement freezes or on the other hand melts previously accreted ice.

There are different methods to study the ice accretion on railway overhead lines that includes, numerical simulations, lab based and field experiments. From last few decades CFD based numerical simulation methods have played an important part for simulation of icing on structures. Numerical simulations of atmospheric ice accretion include the computation of the mass flux of icing particles as well as the determination of the icing conditions. This can be numerically simulated by means of integrated thermo-fluid dynamic models, which requires the use of various coupled numerical tools to obtain the aerodynamics flow field, the droplet's behavior, surface thermodynamics, and phase change. Ice accretion depends on both the geometric design of structures as well as atmospheric parameters such as liquid water content, cloud droplet size, atmospheric temperature, and wind speed [14].

Study of ice accretion on conventional power transmission lines has a long history. In 1970's, Wakahama and Kuroiwa studied the process of accretion of wet snowflakes on electric wires [19]. Makkonen's work of 1984 about modeling of ice accretion on powerline conductors is one of the pioneers' works, where he used a time- dependence numerical model to simulate the amount of accreted ice on wires [20]. Causes, mechanism, and dynamic of ice accretion on power transmission wires has been evaluated in different studies, using different methods [21-27]. Fu and Farzane developed a numerical model to simulate the ice accretion on wires and tested it using several experiments in the wind tunnel [28]. In 2009, Musilek et al. developed an Ice Accretion Forecasting System (IAFS) for power transmission lines. In this system, they used a mesoscale, a numerical weather prediction model, a precipitation type classifier, and an ice accretion model [29-31].

Some investigations about ice accretion on railway contact wires are also done. It should be considered that there are differences between railway contact wires and electric transmission line conductors that make it necessary to work on the railway lines separately. Electrical transmission lines often consist of steel-cored aluminum strands, span great distances (300–500 m) between towers, while railway contact wires are mostly made of copper alloys and have many bearing points in short span (less than 65m) and droppers(8-12m). The height of these wires is usually six meters above the ground [16]. Also, both conductors have different geometric shapes and sizes. Figure 2 shows two different shapes of conductors. Most of conductors in overhead system of railways are similar to Shape (b).

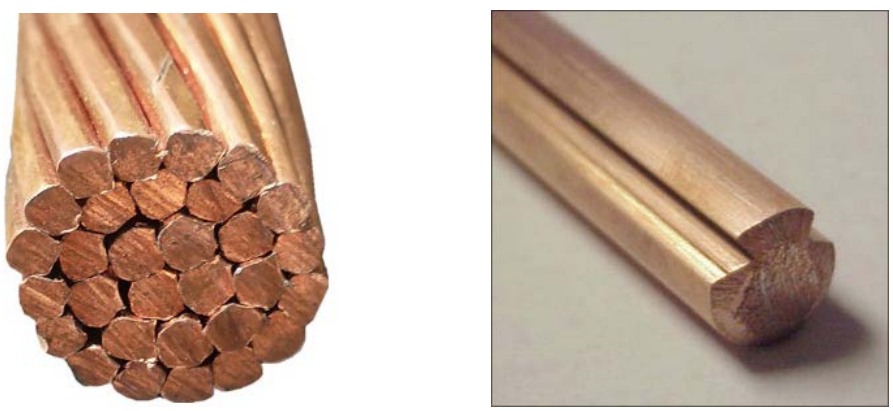

(a) (b)

Figure 2: (a) Circular and (b) Grooved overhead lines conductors.

In 2003, an ice-prediction model was developed to provide short-period forecasts of ice on railway contact wires. It was a statistical model that provided forecasts of wire surface temperature and state (ice or no ice) for three hours ahead. Additionally, forecasts included air temperature, dew point, and wind speed. Validation of results shows slight bias in predicting wire surface temperature, air temperature, dew point, and wind speed [32]. In 2012, in an experimental study the effect of wind speed, atmospheric temperature, and LWC on ice accretion and melting was evaluated. In this research two different cross-sections were studied, the grooved shape and the circular. After the measurement of accreted ice masse from experiments, it was compared with the ice accretion model of Imai at different air velocities [16]. Hong et, al in 2017 provided a synergetic damage recognition approach for the messenger wire in icing environment. This technique offers a real-time online identification for the damage of the messenger wire [33].In a statistical work, Mati and his colleagues tried to find the probability of ice formation on overhead lines. Using ProRail reports and weather data, the authors tried to find a model to estimate the daily probability of ice accretion on overhead wires in Dutch railway. They found that air temperature, relative humidity, and dew point are significant factors in the model. Some researchers also studied about anti-icing methods for railway contact wires, Nilssen et,al. investigated that how resistive heating can be used for preventing ice accretion on metallic electrical cables. They used a circular profile of 12mm diameter and performed experiments at wind speed of 2.5 m/sec and temperatures -5, -10°C in a climate chamber [14]. In another work, a new configuration of the supply system and of the traction line was proposed to make a current circulation in the overhead contact wires during the nighttime to keep the wires ice free [34].

Although there are some published research works about dynamics of railway catenary systems during ice accretion [35, 36], but still not much work has been done to study the ice accretion physics on railway overhead contact wires. This paper focuses on studying the ice accretion on railway overhead line conductors using the multiphase numerical simulations, where two different geometric shape conductors of 12 mm diameter, 1) a grooved shape contact wire (like an actual railway conductor); 2) a circular shape contact wire are used. Computational Fluid Dynamics (CFD) based numerical simulations are carried out for both geometric configurations at different operating parameters such as wind speed, Liquid Water Content (LWC), cloud droplet size distribution, and atmospheric temperature.

2. METHODOLOGY

To examine the airflow and droplet behavior and resultant ice accretion at various operating and geometric conditions, numerical analyses are carried out using ANSYS FENSAP-ICE. This software is widely used for ice accretion studies for different applications [37]. These simulations provided an insight overview of the airflow and droplet behavior, which is not easy to study from experiments. Atmospheric ice accretion on railway contact wires is numerically simulated by means of integrated thermo-fluid dynamic models, which involve the fluid flow simulation, droplet's behavior, surface thermodynamics and phase changes. Airflow behavior is simulated by solving the nonlinear partial differential equations for the conservation of mass, momentum, and energy.

$$\frac{\partial \rho_\alpha}{\partial t} + \vec{\nabla}(\rho_\alpha \overrightarrow{v_\alpha}) = 0 \tag{1}$$

$$\frac{\partial \rho_\alpha \overrightarrow{v_\alpha}}{\partial t} + \vec{\nabla}(\rho_\alpha \overrightarrow{v_\alpha}\,\overrightarrow{v_\alpha}) = \vec{\nabla}.\sigma^{ij} + \rho_\alpha \vec{g} \tag{2}$$

$$\frac{\partial \rho_\alpha E_\alpha}{\partial t} + \vec{\nabla}(\rho_\alpha \overrightarrow{v_\alpha} H_\alpha) = \vec{\nabla}\left(\kappa_\alpha(\vec{\nabla} T_\alpha) + v_i \tau^{ij}\right) + \rho_\alpha \vec{g} \overrightarrow{v_\alpha} \tag{3}$$

In these equations, the density of air is denoted by ρ, v is the velocity vector, subscript α refers to the air solution, air static temperature in Kelvin is represented with T. E and H are the total initial energy and enthalpy, and σ^{ij} is the stress tensor. The Eulerian method is used to model two-phase flow (air and water droplets), with the assumption that the super-cooled water droplets are spherical. The Navier Stokes equation with the water droplet continuity and momentum equation makes up the Eulerian two-phase fluid model.

$$\frac{\partial \alpha}{\partial t} + \vec{\nabla}\left(\alpha \overrightarrow{V_d}\right) = 0 \tag{4}$$

$$\frac{\partial (\alpha \overrightarrow{V_d})}{\partial t} + \vec{\nabla}\left(\rho_\alpha \overrightarrow{V_d} H_d\right) = \frac{C_D Re_d}{24 k \alpha (\overrightarrow{V_\alpha} - \overrightarrow{V_d})} + \frac{\alpha\left(1 - \frac{\rho_\alpha}{\rho_d}\right)1}{Fr^2 \vec{g}} \tag{5}$$

Here α is the water volume fraction and the droplet velocity is represented by V_d, C_D is the droplet drag coefficient, ρ_d is droplet's density, ρ_α is air density and Fr is the Froude number. The droplet behaviour is primarily governed by its Reynolds number and droplet's inertia parameter k, which shows the "balance" of inertial and drag forces, acting on it. The "inertia" of the droplet can be estimated using the droplet's inertia parameter, k, which is also a definition of Stokes number. the droplet's drag coefficient C_D has a non-linear scaling with "Red", and it tends to decrease as the droplet's Reynolds number increases. For example, FENSAP-ICE uses the following empirical fit for the droplet's drag coefficient:

$$C_D = \left(\frac{24}{Re_d}\right)(1 + 0.15 Re_d^{0.687}) \qquad \text{for} \qquad Re_d \leq 1300 \tag{6}$$

$$C_D = 0.4 \qquad \text{for} \qquad Re_d \leq 1300 \tag{7}$$

This parameterization shows that as "Re_d " increases the drag coefficient C_D will decrease, until it reaches the lower bound of $C_D = 0.4$. The decrease in the droplet's drag will, in turn, decrease the droplet's deceleration, thus allowing them to impinge on the object more easily.

The numerical study is conducted at a fixed droplet median volume diameter using Langmuir D distribution spectrum. The calculation of surface thermodynamics considers the heat flux resulting from convective and evaporative cooling, heat of fusion, viscous and kinetic heating, as well as the mass and energy conservation equations. Here the partial differential equation on solid surfaces for the conservation of mass is presented:

$$\rho_f \left[\frac{\partial h_f}{\partial t} + \vec{\nabla}(\overline{V_f} h_f)\right] = V_\infty LWC\beta - \dot{m}_{evap} - \dot{m}_{ice} \tag{8}$$

$$\rho_f \left[\frac{\partial h_f c_f \dot{T}_f}{\partial t} + \dot{\nabla}\left(\partial h_f c_f \dot{T}_f\right)\right] = \left[c_f\left(\tilde{T}_\infty - \tilde{T}_f\right) + \frac{\overrightarrow{V_d}^2}{2}\right] V_\infty LWC\beta - L_{evap}\dot{m}_{evap} + \left(L_{fusion} - c_s \tilde{T}\right)\dot{m}_{ice} + \sigma\varepsilon\left(T_\infty{}^4\right) - T_{f^4} - c_h\left(\tilde{T}_f - \tilde{T}_{ice,rec}\right) + Q_{anti-icing} \tag{9}$$

Physical properties of the fluid and of the solid are presented by ρ_f, c_f , c_s, σ_ε, L_{evap}, L_{fusion}. The reference conditions T_∞, V_∞, LWC are the airflow and droplets parameters. 3D grid is generated by extruding a single cell layer in the span wise direction. ALE (Arbitrary Lagrangian Eulerian) formulation is used for the grid displacement during ice accretion, which adds the grid speed terms to the Navier-Stokes equations to account for the mesh velocity.

In this study, two different geometric shapes are used as contact wire profiles. The circular shape and grooved shape. Mesh sensitivity study was carried out using coarse, medium, and fine meshes to accurately determine the boundary layer characteristics (shear stress and heat flux). For each case, the mesh was automatically displaced after each time shot to account for the ice growth without any change in mesh size. During mesh sensitivity analysis, number of mesh elements and y+ value < 1 for first cell layer was selected based upon the heat flux calculations, where a numerical check was imposed that the heat flux computed with the classical formulae $\frac{dT}{dn}$ should be comparable with the heat flux computed with the Gresho's method. An O type structured numerical grid is used with the size of smallest element in both grids is 10^{-6} (Figure 3). K-omega SST turbulence model is used as a compromise between acceptable computational cost and required accuracy for simulating the turbulent flow. Sand grain roughness height for the iced surface was calculated with an empirical correlation described by Shin and Bond.

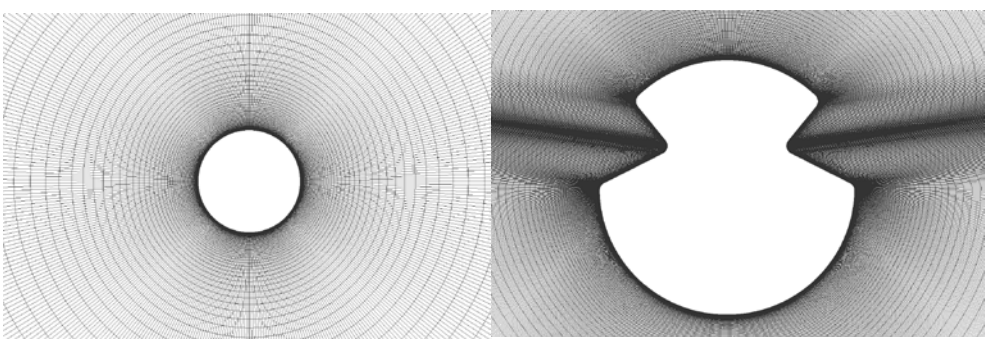

(a) (b)

Figure 3: Numerical mesh for powerline conductors used in this study: (a) circular (b) grooved shape.

Table 2: Operating conditions used for simulations.

Conductor diameter (mm)	**12**
Conductor shape	Grooved & Circular
Droplet size, MVD (μm)	20
Liquid Water Content, LWC(g/m3)	0.25, 1
Wind velocity (m/s)	10, 25
Atmospheric air temperature (°C)	-2, -25
Angle of attack (degree)	0
Icing duration (min)	20

3. RESULTS & DISCUSSION

3.1. Validation of Numerical Model

Not much work has been carried out (so far) by the researchers to study the icing on railway overhead powerline conductors. Most of the previous work has focused on the circular overhead transmission line conductors. CFD model used in this study is validated with the experimental data obtained from the circular overheard power line conductors. No experimental data is publicly available for scientific validation of the icing on grooved shape railway overhead power line conductors. The numerical setup used in this work is validated with the experimental data from icing tunnel experiments about icing on circular overhead powerline conductors. This experimental data was obtained from the research article published by Ping Fu et al. [28]. After finding a good agreement with the published experimental results, the same numerical setup is used to study icing on grooved railway overhead power line conductors. Following figure 4 shows the comparison of numerical simulated ice shape along circular overhear power lines with the experimental data.

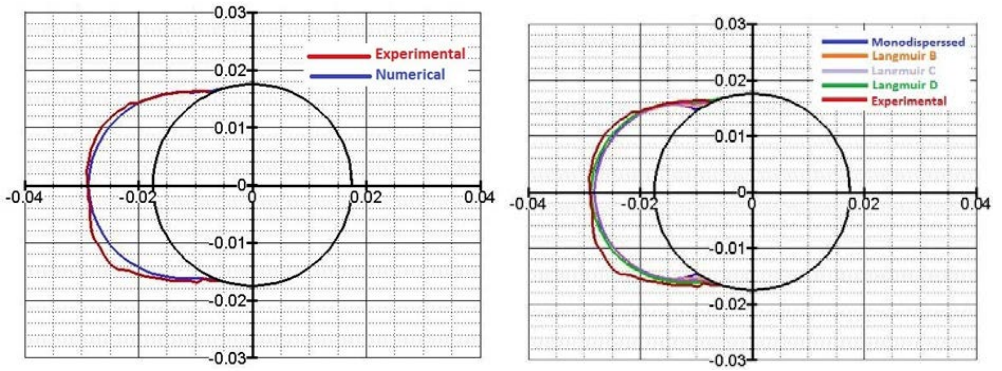

Figure 4: Validation of ice shape with experimental data

3.2. Effect of Wind Velocity

To study the effects of wind velocity, simulations are carried at two different wind velocities (10 & 25 m/s). This parametric study is carried out at a constant air temperature of -25°C, MVD of 20 µm for Langmuir- D droplet distribution, LWC 0.25 g/m^3 and an incoming wind angle of attack of 0°. Results show that the wind velocity effect the airflow behavior around conductor, which also affects the droplet collision and resultant ice accretion. For grooved shape conductor, a wake region is observed in the concavity area along windward side of the grooved conductor, whereas for circular shape conductor no flow separation is observed along windward side. At leeward side of both conductors a significant flow separation is observed which is more prominent in case of grooved shape conductor. Figure 5 shows the velocity streamline for both cases.

Supercooled water droplet moving in the free stream air is influenced by its drag and inertia, when neglecting the gravity and buoyancy. If drag dominates the inertia, the droplet follows the streamline whereas, for the case where inertia dominates, the droplet collides with the airfoil surface. The ratio of droplet inertia to drag depends on the wind velocity. Results show an increase in the droplet collision efficiency with the increase of wind velocity for both

conductors. This is mainly due to an increase in the droplet inertia and leads to an increase in the droplet collision efficiency [38]. Figure 6 shows a comparison of droplet collision efficiency for circular and grooved shape conductors at both wind velocities.

Results show that in case of circular conductor the maximum collision efficiency is observed along the stagnation point on the windward side of the conductor, whereas for the grooved shape conductor due to flow wake/separation in the concave section, not many droplets impinge there due to which a low droplet collision efficiency is observed. Most of the droplets impinged at the outer corners of the concave section. Similar behavior of droplet impingement is observed for both the wind velocities. This has led to higher accreted ice thickness and mass at the location of higher droplet impingement. Figure 7 shows the resultant ice shape for both geometric configurations at t= 20 minutes. Results show an increase in ice thickness and mass with the increase of wind velocity.

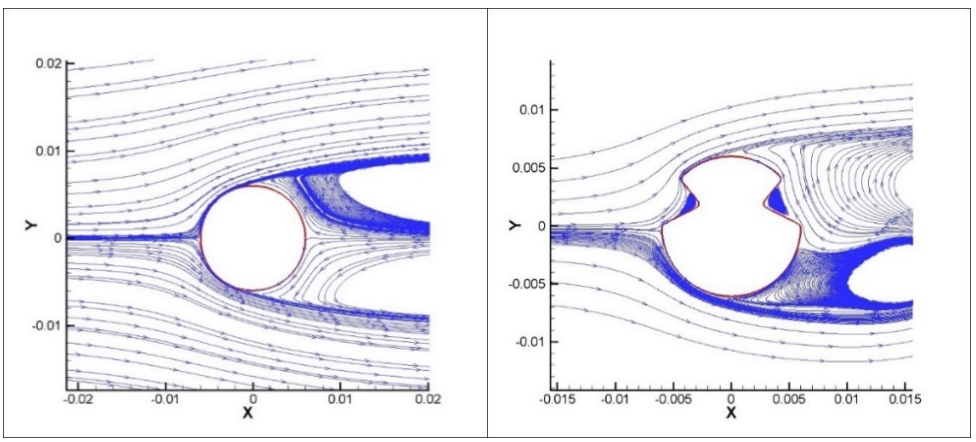

(a) (b)

Figure 5: Velocity streamline for (a) Circular and, (b) Grooved shape conductors.

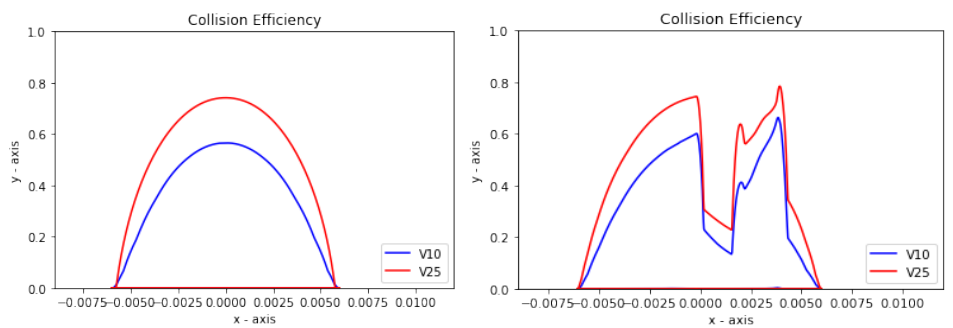

(a) (b)

Figure 6: Effect of wind velocity on droplet collision efficiency: (a) circular (b) grooved shape.

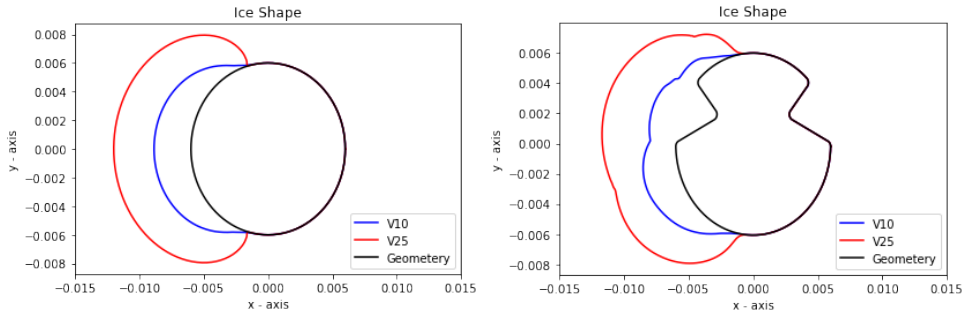

(a) (b)

Figure 7: Effect of wind velocity on ice accretion: (a) circular and (b) grooved shape.

3.3. Effect of Atmospheric Temperature

To study the effect of atmospheric temperature, numerical analyses are carried out at two different atmospheric temperatures (-2 and -25°C). This parametric study is carried out at a constant wind velocity of 10 m/s, MVD of 20 microns for Langmuir D droplet distribution, LWC of 0.25 g/m^3 and an incoming air flow angle of attack of 0 degrees. Results show that accreted ice shape changes with the air temperature. The change in air temperature has no effect on the droplet collision efficiency, but the rate and shape of ice changes with the air temperature mainly due to change of surface heat fluxes. At very low temperatures, such as -25°C, the droplet freezing fraction is almost 100%. Because of this, all colliding droplets freeze into ice. For higher temperature, such as -2°C, the droplet freezing fraction is lower than 100% due to which most of the colliding droplets do not freeze along the conductor surface and run back as thin layer of water. Such change in the droplet freezing fraction due to surface heat fluxes results in different ice accretion process and results in different accreted ice densities [38]. Figures 8 and 9 show the effect of temperature variation on droplet collision efficiency and resultant ice accretion.

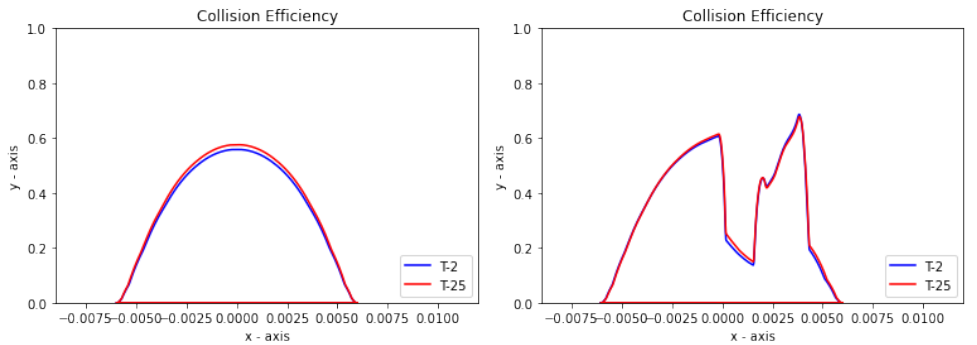

(a) (b)

Figure 8: Effect of temperature on droplet collision efficiency: (a) circular (b) grooved shape.

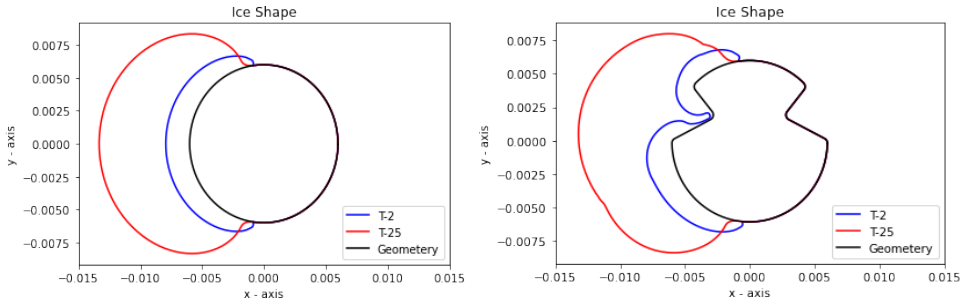

(a) (b)

Figure 9: Effect of temperature on ice accretion: (a) circular (b) grooved shape.

The analyses show that temperature has no effect on the droplet collision efficiency, but it has a significant effect on results ice mass and thickness. Ice mainly accretes along windward side of both conductors. For rime ice condition at -25°C the accreted ice thickness is higher than the ice accretion at -2°C. For circular conductor, more streamlined ice shapes are observed as compared to the grooved shape conductor. Especially at -2°C in case of grooved shape conductor, the ice is also accreted in the concave section. This is possibly due to water run back at -2°C. Complex accreted ice shapes can change the flow behavior and the resultant aerodynamic characteristics of the conductor especially in case of galloping.

3.4. Effect of Liquid Water Content

To study the effect of liquid water content on ice accretion, analyses are carried out at two LWC values, 0.25 & 1 g/m^3. Liquid water content is defined as the quantity of water contained in a volume of air [39]. Analysis shows that change in LWC significantly effects the ice accretion. At higher values of LWC, more water is present in the air, which can lead to increased ice accretion. Figure 10 shows that for both geometric configurations, the ice thickness increased with the increase of LWC.

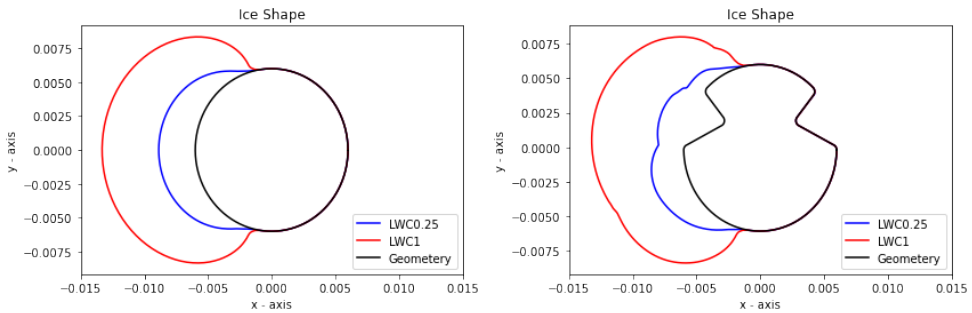

(a) (b)

Figure 10: Effect of LWC variation on ice accretion: (a) Circular and (b) Grooved shape.

3.5. Effect of Droplet Distribution Spectrum and Droplet Size

A detailed parametric study was carried out to understand the effect of droplet distribution spectrums on droplet collision efficiency and resultant ice accretion. Analysis was carried out at MVD of 20 microns, air velocity of 10m/sec, LWC of 0.25 and -25°C as temperature using Langmuir distributions. Results show that, the droplet collision efficiency changes with the change of the droplet distribution spectrum. For both geometric configurations, the maximum collision efficiency was recorded for monodisperse distribution spectrum (Lang-A). Also, the shape of ice in Lang A is different from other spectrums. Although for the circular conductor, the droplet collision efficiency changes in a sequence from Lang A to E, in the grooved geometry the droplet collision efficiency did not follow a pattern. Figure 11 shows the droplet collision efficiency and resultant ice accretion for Lang A-E spectrums.

Table 3: Distribution of droplets size in each Langmuir

	5%	10%	20%	30%	20%	10%	5%
Droplet size in Lang A(µm)	Monodisperse (20 µm)						
Droplet size in Lang B(µm)	49	46.20	40.95	35	29.40	25.20	19.60
Droplet size in Lang C(µm)	63.35	52.85	44.10	35	26.95	21.35	14.70
Droplet size in Lang D(µm)	77.70	60.90	47.95	35	24.85	18.20	10.85
Droplet size in Lang E(µm)	94.85	70	51.80	35	22.75	15.40	8.05

The weight of each droplet size in various lang is shown in Table 3. Since Lang A is monodisperse, all the droplets have a diameter of 20 microns. The percentage of larger droplets grows from lang B to lang E, as does the size difference between the largest and smallest droplets.

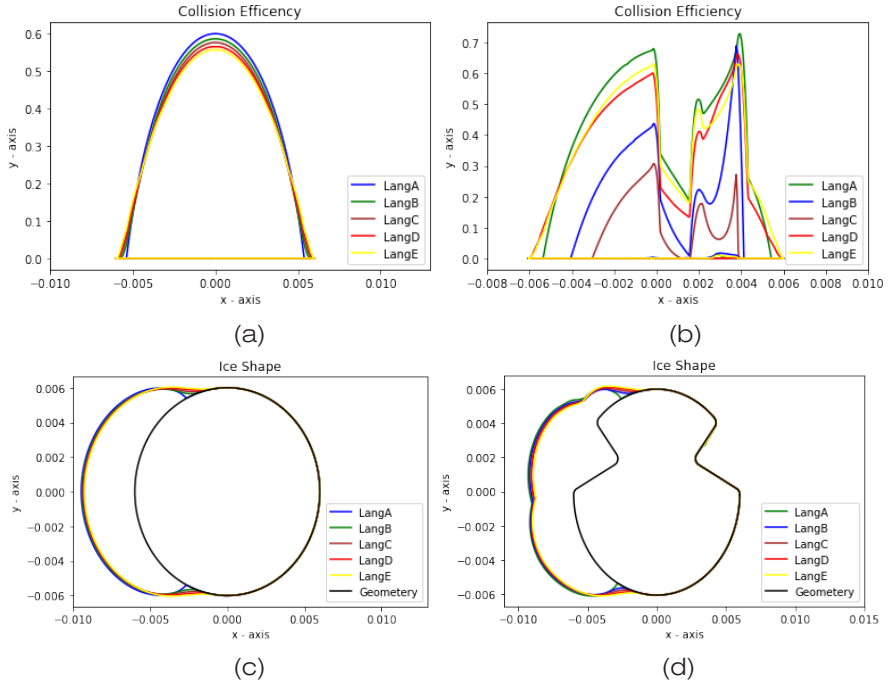

Figure 11: Effect of droplet distribution spectrum on ice shape and droplet collision efficiency: (a & c) Circular and (b & d) Grooved shape.

A study was also carried out to understand the effect of droplet size (MVD) by keeping air velocity, temperature, LWC constant. Different MVD's were analyzed using Lang D distribution spectrum. Results show that the droplet size has a direct relation with the droplet collision efficiency and consequently with the ice mass. Larger droplets are less vulnerable to change their direction in an airflow, so more droplets can collide the contact wire surface. Figure 12 shows the droplet collision efficiency and resultant ice shape.

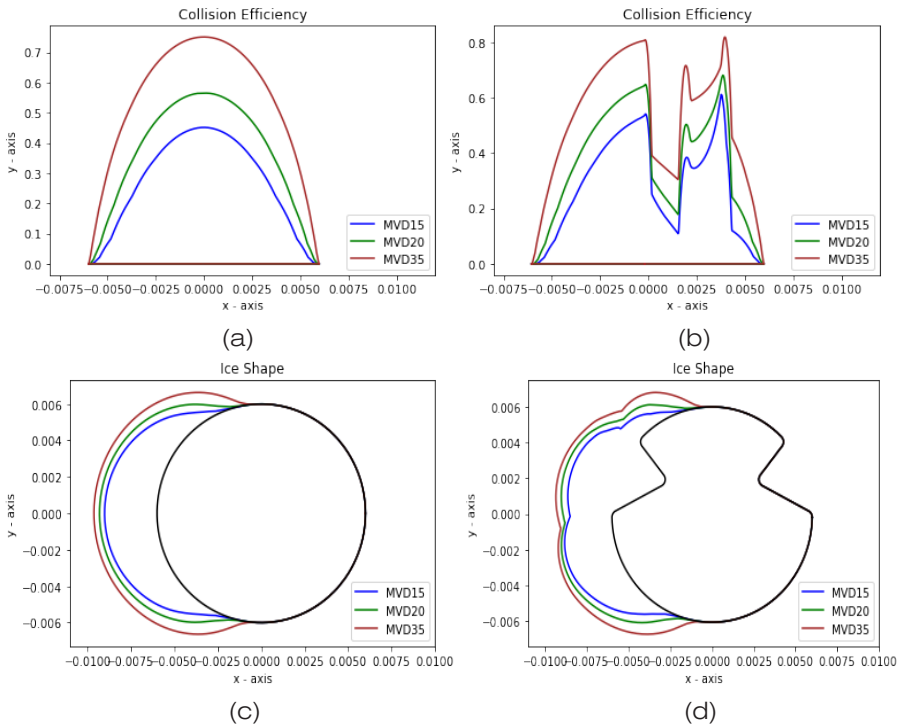

Figure 12: Effect of droplet size on ice shape and droplet collision efficiency: (a & c) circular and (b & d) grooved shape.

4. CONCLUSION

The numerical study presented in this paper shows that both operating and geometric parameters affect the rate and shape of ice accretion on overhead powerline conductors. Grooved shape conductor, which is being used in railway overhead power infrastructure has more irregular accreted ice shapes as compared to the circular conductor, which can lead to complex flow behavior and aerodynamic performance penalties. Analysis shows that an increase in wind velocity, LWC, MVD, and a decrease in air temperature leads to an increase in accreted ice mass and thickness. Increase in wind velocity also leads to higher values of droplet collision efficiency which results in more ice accretion, whereas decrease in air temperature leads to increase in droplet freezing fraction which also results in increased ice accretion. This numerical study provided a base knowledge about atmospheric ice accretion on railway overhead powerline conductors, but still further analyses are required with the help of lab experimentation and field measurements.

ACKNOWLEDGEMENT

The work reported in this paper is supported by nICE project (Project no- 324156) funded by UiT & Research Council of Norway.

REFERENCES

[1] Rossetti, M.A. Potential Impacts of Climate Change on Railroads 2003. https://www.transportation.gov/sites/dot.gov/files/docs/rossetti_CC_Impact_Railroads.pdf

[2] WeatherSpark, The Weather Year-Round Anywhere on Earth. 2022, Accessed date: 15.10.2022. https://weatherspark.com/

[3] Garmabaki, A.H.S., et al. Adapting Railway Maintenance to Climate Change. Sustainability, 2021. 13(24).

[4] Garcia-Marti, I, et al. Detecting probability of ice formation on overhead lines of the dutch railway network. in 2018 IEEE 14th International Conference on e-Science (e-Science). 2018.

[5] Kostianaia, E.A., et al. Impact of Regional Climate Change on the Infrastructure and Operability of Railway Transport. Transport and Telecommunication Journal, 2021. 22(2): p. 183-195.

[6] Nemry, F; H. Demirel. Impacts of Climate Change on Transport: A focus on road and rail transport infrastructures 2012, Joint Research Centre Institute for Prospective Technological Studies: Luxembourg

[7] Palin, E, et al. Implications of climate change for railway infrastructure. WIREs Climate Change, 2021. 12.

[8] Tahvili, N. Winterization of Railways Issues and Effects, Department of Industrial Economics and Technology Management. 2016, Norwegian University of Science and technology Institute of Production and Quality Engineering. p. 162.

[9] Thaduri, A; Garmabaki, A; Kumar, U. Impact of climate change on railway operation and maintenance in Sweden: A State-of-the-art review. Maintenance, Reliability and Condition Monitoring, 2021. 1(2): p. 52-70.

[10] Stenström, C, et al., Impact of cold climate on failures in railway infrastructure, in The 2nd International Congress on Maintenance Performance Measurement & Management Conference Proceedings. 2012.

[11] Thornes, J.E; Davis B.W. Mitigating the impact of weather and climate on railway operations in the UK. in ASME/IEEE Joint Railroad Conference. 2002.

[12] Zakeri, G; Olsson, N.O.E, Investigating the effect of weather on punctuality of Norwegian railways: a case study of the Nordland Line. Journal of Modern Transportation, 2018. 26(4): p. 255-267.

[13] Xu, Z; Song, Y; Liu, Z, Effective Measures to Improve Current Collection Quality for Double Pantographs and Catenary Based on Wave Propagation Analysis. IEEE Transactions on Vehicular Technology, 2020. 69(6): p. 6299-6309.

[14] Nilsson, F, et al., Modelling anti-icing of railway overhead catenary wires by resistive heating. International Journal of Heat and Mass Transfer, 2019. 143: p. 118505.

[15] Solangi, A.R., Icing Effects on Power Lines and Anti-icing and De-icing Methods, in Department of Safety and Engineering. 2018, UIT The Arctic University of Norway

[16] Heyun, L; Xiaosong, G; Wenbin, T. "Icing and Anti-Icing of Railway Contact Wires", in Reliability and Safety in Railway. 2012, London, United Kingdom: IntechOpen.

[17] Er, U; Çakir, F. Urban Light Rail Transportation Systems Catenary Line Anti-Icing Applications, Laboratory and Field Tests. Anadolu University Journal of Science and Technology-A Applied Sciences and Engineering, 2018. 19: p. 433-442.

[18] Postojna, Ž. Railway Transport Union of Slovenia. http://www.sindikat-szps.si/2014/02/04/zled-na-nasi-zeleznici/zled-postojna-prestranek-pivka-32/.

[19] Wakahama, G; Kuroiwa, D; Gotō, K. Snow Accretion on Electric Wires and its Prevention. Journal of Glaciology, 1977. 19(81): p. 479-487.

[20] Makkonen, L. Modeling of Ice Accretion on Wires. Journal of Applied Meteorology and Climatology, 1984. 23(6): p. 929-939.

[21] Jones, K.F; Egelhofer K.Z. Computer model of atmospheric ice accretion on transmission lines. Cold Regions Research and Engineering Laboratory 1991.

[22] Liu, C.C; Liu, J. Ice Accretion Cause and Mechanism of Glaze on Wires of Power Transmission Lines. Advanced Materials Research, 2011. 189-193: p. 3238-3242.

[23] Personne, P; Gayet, J.F; Ice Accretion on Wires and Anti-Icing Induced by Joule Effect. Journal of Applied Meteorology and Climatology, 1988. 27(2): p. 101-114.

[24] Niu, S.J, et al. The microphysics of ice accretion on wires: Observations and simulations. Science China-Earth Sciences, 2012. 55(3): p. 428-437.

[25] Fu, P; Farzaneh, M. Simulation of the ice accretion process on a transmission line cable with differential twisting. Canadian Journal of Civil Engineering, 2007. 34(2): p. 147-155.

[26] Hu, J, et al. Numerical Simulation of Iced Conductor Galloping, International Conference on Material Science and Civil Engineering, MSCE 2016. 2016. p. 611-617.

[27] Muller, M; Muller, Z; Tlusty, J. Icing Influence Simulation Using 3-DOF Overhead Line Modelling, Proceedings of 2015, 16TH International Scientific Conference on Electric Power Engineering (EPE). 2015. p. 381-384.

[28] Fu, P; Farzaneh, M; Bouchard, G. Two-dimensional modelling of the ice accretion process on transmission line wires and conductors. Cold Regions Science and Technology, 2006. 46(2): p. 132-146.

[29] Musilek, P; Arnold, D; Lozowski, E.P. An Ice Accretion Forecasting System (IAFS) for Power Transmission Lines Using Numerical Weather Prediction. SOLA, 2009. 5: p. 25-28.

[30] Kozlovskyi, O, et al. Icing Sensor on the Overhead Powerlines Wires, in 2015 16th International Conference on Computational Problems of Electrical Engineering (CPEE). 2015. p. 88-91.

[31] Gubeljak, N, et al. Preventing Transmission Line damage caused by ice with smart on-line conductor Monitoring. in 2016 International Conference on Smart Systems and Technologies (SST). 2016.

[32] Shao, J, et al. Nowcasts of temperature and ice on overhead railway transmission wires. Meteorological Applications, 2003. 10(2): p. 123-133.

[33] Hong, X, et al. Synergetic damage recognition approach for messenger wire in icing environment using piezoceramic transducers. Measurement, 2018. 122: p. 522-531.

[34] Cinieri, E; Fumi, A. Deicing of The Contact Lines of the High-Speed Electric Railways: Deicing Configurations. Experimental Test Results. IEEE Transactions on Power Delivery, 2014. 29(6): p. 2580-2587.

[35] Wang, S, et al. Multiphysics simulation and shed structure optimization of catenary icing insulator. Archives of Electrical Engineering, 2021. 70(3): p. 675-688.

[36] Yao, Y, et al. Dynamic Analysis of Pantograph-Catenary System considering Ice Coating. Shock and Vibration, 2020.

[37] Muhammed, M; Virk, M.S. Ice Accretion on Fixed-Wing Unmanned Aerial Vehicle; A Review Study. Drones, 2022. 6(4): p. 86.

[38] Jin, J.Y; Virk, M.S. Study of ice accretion along symmetric and asymmetric airfoils. Journal of Wind Engineering and Industrial Aerodynamics, 2018. 179: p. 240-249.

[39] De Florio, F. Chapter 4 - Airworthiness Requirements, in Airworthiness (Third Edition), F. De Florio, Editor. 2016, Butterworth-Heinemann. p. 37-83.